Graduate School of Oceanography Faculty
Publications

Graduate School of Oceanography

A Numerical Investigation of Land Surface Water on Landfalling Hurricanes

Weixing Shen
University of Rhode Island

Isaac Ginis
University of Rhode Island

Robert E. Tuleya

Follow this and additional works at: https://digitalcommons.uri.edu/gsofacpubs

A Numerical Investigation of Land Surface Water on Landfalling Hurricanes

Terms of Use

A Numerical Investigation of Land Surface Water on Landfalling Hurricanes

Weixing Shen and Isaac Ginis

Graduate School of Oceanography, University of Rhode Island, Narragansett, Rhode Island

Robert E. Tuleya

NOAA Geophysical Fluid Dynamics Laboratory, Princeton, New Jersey

ABSTRACT

Little is known about the effects of surface water over land on the decay of landfalling hurricanes. This study, using the National Oceanic and Atmospheric Administration Geophysical Fluid Dynamics Laboratory hurricane model, examines the surface temperature changes due to hurricane–land surface water interactions, and their effects on the surface heat fluxes, hurricane structure, and intensity. Different water depths and surface conditions are incorporated for a variety of experiments starting with a hurricane bogus embedded in a uniform easterly mean flow of 5 m s^{-1}.

A salient feature of hurricane–land surface water interaction is the local surface cooling near the hurricane core with the largest cooling behind and on the right side of the hurricane center. Unlike the surface cooling due to hurricane–ocean interaction, the largest cooling in hurricane–land surface water interaction can be much closer to the hurricane core. Without solar radiation during night, the surface evaporation dominates the local surface cooling. This causes a surface temperature contrast between the core area and its environment. During the day, the surface temperature contrast is enhanced due to additional influence from the reduced solar radiation under the core. Related to the local surface cooling, there is a significant reduction of surface evaporation with a near cutoff behind the hurricane center. A layer of half-meter water can noticeably reduce landfall decay although the local surface temperature around the hurricane core region is more than 4°C lower than in its environment. Further experiments indicate that an increase of roughness reduces the surface winds but barely changes the surface temperature and evaporation patterns and their magnitudes since the increase of roughness also increases the efficiency of surface evaporation.

1. Introduction

One of the known facts about landfalling hurricanes is their rapid decay; yet some of them retain tropical storm winds and gusts well inland. Both observational and modeling studies (e.g., Miller 1964; Tuleya and Kurihara 1978) revealed that the reduction of surface evaporation is critical to hurricane decay during landfall. However, little has been known about the role of land surface water, which can be more than 1 m deep in swampy/marshy and flooded areas, in effecting landfall decay.

Early hurricane modeling studies of sensitivity of hurricane development and intensity to sea/land surface conditions (e.g., Ooyama 1969; Rosenthal 1971) were performed through alterations of *the exchange coefficients* of heat, moisture, and momentum at the surface. These studies found that tropical cyclones failed to develop and be maintained if the exchange coefficients were reduced to relatively small values. Subsequent studies of Tuleya and Kurihara (1978) and Tuleya et al. (1984) differentiated the relative roles of surface evaporation cutoff and increased friction for landfalling hurricanes.

All the above numerical investigations used fixed underlying surface conditions. However, hurricane interaction with underlying surface results in changes of the underlying surface characteristics, in particular change of the surface evaporation, the primary energy source for hurricanes. Hurricane intensity is thus effected by surface feedback mechanisms both over land and water, which cause surface cooling. In hurricane–ocean interaction, it is mainly the hurricane-induced turbulent mixing in the upper ocean and entrainment of colder water under the mixed layer, that leads to sea surface cooling (e.g., Sutyrin 1980; Bender et al. 1993; Ginis 1995). The largest surface cooling occurs behind and on the right side of the hurricane due to hurricane movement and the Coriolis force (Price 1981). For landfalling hurricanes over a moist land, surface evaporation is a self-limiting process. This is because for a limited heat capacity of soil, any increase of evaporation yields a surface cooling that limits further evaporation. Tuleya (1994), using the Geophysical Fluid Dynamics Labo-

Corresponding author address: Weixing Shen, NCEP/EMC Room 207, 5200 Auth. Rd., Camp Springs, MD 20746.
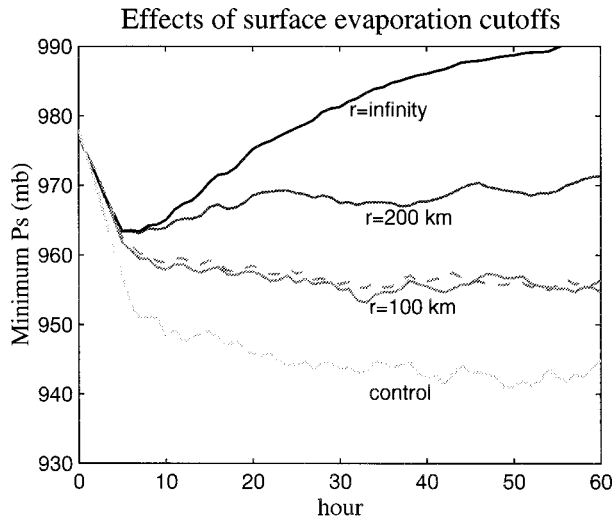E-mail: weixing.shen@noaa.gov

FIG. 1. Model-attained minimum surface pressures for the experiments with idealized surface evaporation cutoffs over the ocean with a fixed SST. The evaporation cutoffs are axisymmetric about the hurricane center within specified radius r. The dashed curve gives the results with both surface evaporation and sensible heat flux cutoffs in the area within $r = 100$ km.

TABLE 1. Experiments for idealized surface flux cutoffs.

Radius of the cutoff	Evaporation cutoff	Sensible heat cutoff
0 (control case)	No	No
100 km	Yes	No
100 km	Yes	Yes
200 km	Yes	No
Infinite	Yes	No

* Ocean surface albedo is set to be 0.06.

surface roughness conditions are considered. An experiment with inhomogeneous surface water depths is also conducted.

The paper is organized as follows: section 2 describes the hurricane model and experiment design in this study. Section 3 discusses the results of hurricane responses to specified local surface heat flux cutoffs. Section 4 presents the results of the effects of hurricane-induced local surface cooling on landfall decay. In section 5, diurnal variations of land surface water cooling and hurricane intensity are discussed. In section 6, we summarize the main results of this study.

2. Experimental design

a. Review of model

The GFDL hurricane model (Kurihara et al. 1998) with triply nested movable meshes, was used in this study. This model is a primitive equation model formulated in latitude, longitude, and σ coordinates, with 18 levels in the vertical (Kurihara et al. 1990, Table 1). The domains of the three meshes in this study are $75° \times 75°$, $11° \times 11°$, and $5° \times 5°$ with resolutions of $1°$, $1/3°$, and $1/6°$, respectively. The major physical processes included in this model are the cumulus convection treated by the parameterization scheme of Kurihara (1973) with some additional modification (Kurihara and Bender 1980, appendix C), surface flux exchanges by Monin–Obukhov scheme, subgrid-scale horizontal diffusion by the nonlinear viscosity scheme (Smagorinsky 1963), vertical diffusion of the level-2 turbulence closure scheme (Mellor and Yamada 1974) with a background diffusion coefficient added, and the Schwarzkof and Fels (1991) infrared and the Lacis and Hansen (1974) solar radiation parameterizations with diurnal variation and cloud specification.

The bulk subsurface-layer scheme for land surface water temperature prediction is the one used by Tuleya (1994) following Deardorff (1978):

$$\frac{\partial T_L}{\partial t} = \frac{-\sigma T_L^4 - H - \text{LE} + (S + F\downarrow)}{\rho_s c_s d_s}$$
$$- c(T_L - T_{\text{gref}}), \qquad (1)$$

where T_L is the land temperature, $-\sigma T_L^4$ the emission from the earth's surface, H the surface sensible heat flux, LE the surface evaporative heat flux, $(S + F\downarrow)$ the net

ratory (GFDL) hurricane model, investigated the effects of surface coupling on landfalling hurricanes over moist land. He found that the moist land surface coupling, similar to the ocean coupling, tends to reduce the hurricane intensity through local surface cooling, but the mechanisms for the local surface cooling are quite different. Tuleya (1994) also indicated that with a typical soil subsurface layer, the largest surface cooling is near the hurricane center.

The focus of this study is the influence of a land covered by surface water on landfalling hurricanes. The case of water-covered land can be considered to be somewhere between the ocean and wet land conditions. It can be considered as either a horizontally motionless shallow ocean with no vertical temperature gradient or a land of relatively large heat capacity but with a water surface. A bulk subsurface-layer scheme is used to calculate the land surface water temperature. In this study, we attempt to understand: 1) how the land surface water temperature changes under a hurricane, including both the magnitude and pattern of the local surface cooling and their dependence on the surface water depth; 2) what are the major factors that cause the local surface cooling and its diurnal variation; 3) how the local surface cooling effects the decay rate of landfalling hurricanes and why a storm of considerable magnitude can remain even with a large local surface cooling near the hurricane core region. We begin with a set of sensitivity experiments with idealized surface evaporation cutoffs near the hurricane center. We then examine the evaporation-induced local land surface water cooling and its effects on hurricane structure and intensity changes. Different surface water depths, ranging from 8 to 200 cm, and
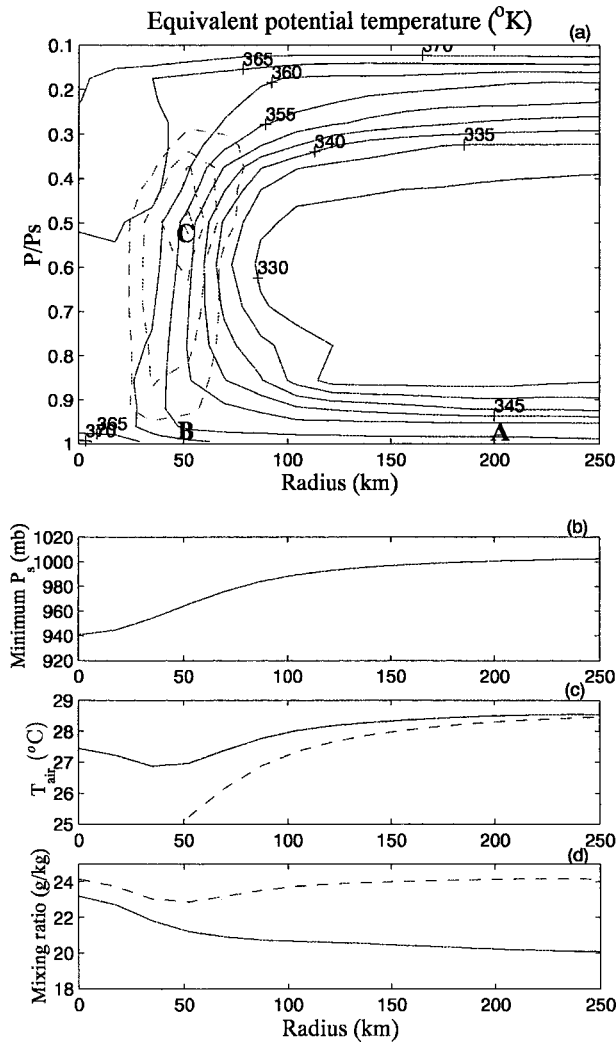
Equivalent potential temperature (°K)

FIG. 2. Axisymmetric (circularly averaged) vertical cross section of θ_e at 50 h and the radial distributions of the associated surface minimum pressure and near-surface (lowest model level) temperature and moisture mixing ratio for the control case. The dashed contours denote the latent heat release with interval of 2 J(kg)$^{-1}$ s^{-1} starting with 2 J(kg)$^{-1}$ s^{-1}. (c) The dashed line shows the temperature of an air parcel moving toward the eyewall adiabatically. (d) The dashed line indicates the saturated mixing ratio.

downward radiative flux at the surface, $\rho_s c_s$ the soil heat capacity, and d_s the damping depth $(\tau \lambda / \rho_s c_s \pi)^{1/2}$, where λ is the thermal conductivity of soil and τ the period of forcing (24 h). The last term for "force-restore" is set to be zero for the short time (60 h) integrations in this study. With heat capacity of 0.5 cal cm^{-3} K^{-1} and thermal conductivity of 0.005 cal cm^{-1} K^{-1} s^{-1}, the soil has a damping depth of about 16.6 cm, which is equivalent to an about 8-cm-deep water (d_w) layer. More generally, the soil heat capacity ($\rho_s c_s$) and damping depth (d_s) in (1) can be replaced by the water heat capacity ($\rho_w c_w$) and equivalent water depth (d_w). In the presence of surface water over land, the equivalent water depth in the bulk subsurface-layer scheme should reflect the
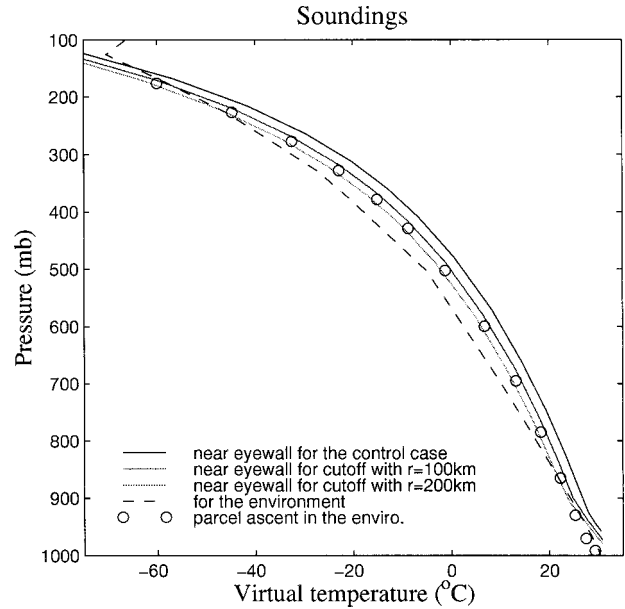

FIG. 3. Various vertical soundings in the cases with idealized surface evaporation cutoffs for the cases of $r = 100$ and 200 km.

combination of the depth of surface water and the property of underlying soil. For convenience, hereafter, the water depth is referred to as the equivalent water depth, the surface-layer heat capacity is referred to as the heat capacity of the whole layer (namely, the product of the water heat capacity $\rho_w c_w$ and the water depth d_w), and the surface temperature is referred to as the subsurface-layer temperature.

b. Classification of experiments

In all experiments, the model was integrated for 60 h starting with various underlying surface conditions. A normal size and deep initial vortex based on Hurricane Fran [see Shen et al. (2000) for details] was used. The initial vortex was centered at $20°N$ with a uniform easterly environmental wind of -5 m s^{-1}. The initial vertical profiles of temperature and relative humidity based on the Global Atlantic Tropical Experiment (GATE III) III tropical conditions were used. These profiles have a surface air temperature of 27.5°C and relative humidity of 84%, respectively. A uniform initial land/sea surface temperature of 28.5°C was used. Except for the different surface conditions, the model initialization of the atmospheric temperature and surface pressure is identical to that of Shen et al. (2000).

In total, three sets of experiments were performed with different underlying surface conditions. The first set investigated the effects of a local surface decoupling of the air–sea interface, using idealized surface flux cutoffs within a circular region of specified radius relative to the hurricane center. An ocean surface with fixed SST of 28.5°C was used in these experiments. Table 1 summarizes these experiments. In the second set of exper-

TABLE 2. Experiments for the effects of surface water over land.

	Equivalent water depth (d_w)	Land surface roughness (Z_o)	Albedo over land (α)	Surface water availability (W)
Hurricane	8 cm[a]	1 cm	0.25	0 (Dry land)
moves from	8 cm	1 cm	0.06	1
sea to land	50 cm	1 cm	0.06	1
	200 cm	1 cm	0.06	1
	8 cm*	10 cm	0.25	0 (Dry land)
	50 cm	10 cm	0.06	1
	200 cm	10 cm	0.06	1
		10 cm	0.06	1
Land surface	8 cm*	1 cm	0.25	0 (Dry land)
everywhere	8 cm	1 cm	0.06	1
	50 cm	1 cm	0.06	1
	100 cm	1 cm	0.06	1
	8–100 cm**	1 cm	0.06	1

* For dry land with soil heat capacity of 0.5 cal cm^{-3} K^{-1} and conductivity of 0.005 cal cm^{-1} K^{-1} s^{-1}.
** With 8 and 100 cm alternatively deep water surface conditions on a resolution of 1/6.

iments, hurricanes were initially placed over ocean and (after about 34 h) encountered a land covered with a water layer. The SST is fixed in the experiments while the surface temperature is predicted based on Eq. (1). The third set of experiments studied the diurnal variations of hurricanes over land covered with water everywhere. The experiments of the second and third sets are summarized in Table 2.

3. Effects of local surface evaporation reduction

Studies of the hurricane–land surface water/ocean couplings basically deal with the effects of surface heat flux reduction related to a phase-lagged local surface cooling on a generally axisymmetric hurricane. The magnitude and structure of the cooling depends on the hurricane size, translation speed, and the underlying surface conditions. Given the small phase lag of surface cooling in the landfall case, the effects of the surface heat flux reduction can conceptually be viewed as the effects of an axisymmetric evaporation reduction around the core region. For a first-order approximation and easier diagnosis, we in this section investigate hurricane responses to idealized local surface flux reductions. In these experiments, uniform fixed sea surface conditions are used with axisymmetric surface heat flux cutoffs within specified distances from the hurricane center (see Table 1).

Figure 1 shows the intensity evolutions with time in these experiments. There is no surface heat flux cutoff in the control case, while evaporation is switched off everywhere in the infinity case. The cutoff of local surface evaporation reduces hurricane intensity but the degree of reduction depends on the size of the cutoff. Tropical storms of considerable magnitudes are maintained with these underlying evaporation cutoffs. The small difference between the solid and dashed curves for the $r = 100$ km case indicates that the influence of the surface sensible heat flux cutoff on hurricane intensity is negligible compared to that of the evaporation

cutoff. The heat flux cutoffs in these experiments were initiated from the beginning but the final states were not dependent on the starting time of the flux cutoffs (not shown).

We now consider the model-attained axisymmetric structure in the control case of fixed surface temperature. Figure 2a shows the height–radius cross section of the equivalent potential temperature θ_e and the diabatic heating due to latent heat release. In the eyewall, air motion in the vertical is nearly moist adiabatic [$\theta_e(B) \sim \theta_c(C)$]. Large radial gradient of θ_e appears in a deep layer near the eyewall where the surface pressure drop is the largest (Fig. 2b). The associated near-surface (lowest model level) air temperature and moisture mixing ratio distributions with respect to radius are shown in Figs. 2c and 2d, respectively. The near-surface air temperature (solid line in Fig. 2c) under the eyewall is seen to be higher than that by an adiabatic expansion but about 1.5°C lower than that of isothermal expansion. The moisture mixing ratio (solid line in Fig. 2d) increases inward about 1 g kg^{-1} from the environment to the eyewall. The decrease of near-surface air temperature and the small increase of the surface mixing ratio toward eyewall are consistent with observations (e.g., Beckerle 1974; Cione and Black 1998; Black and Holland 1995). In the maximum potential intensity theories by Holland (1997) and Emanuel (1995), an isothermal surface inflow is assumed.

Figure 3 shows various virtual temperature soundings in the cases with the surface evaporation cutoffs. As was pointed by several studies (e.g., Riehl 1954; Emanuel 1988), the energy available for hurricane maintenance may be represented by the area between the eyewall sounding and the sounding in the environment. In the control case, the diabatic exchange of the hurricane system with the sea surface is evident from the increased low-level virtual temperature at lower central surface pressures. It contributes a major part of the available hurricane energy. With the surface evaporation cutoffs,
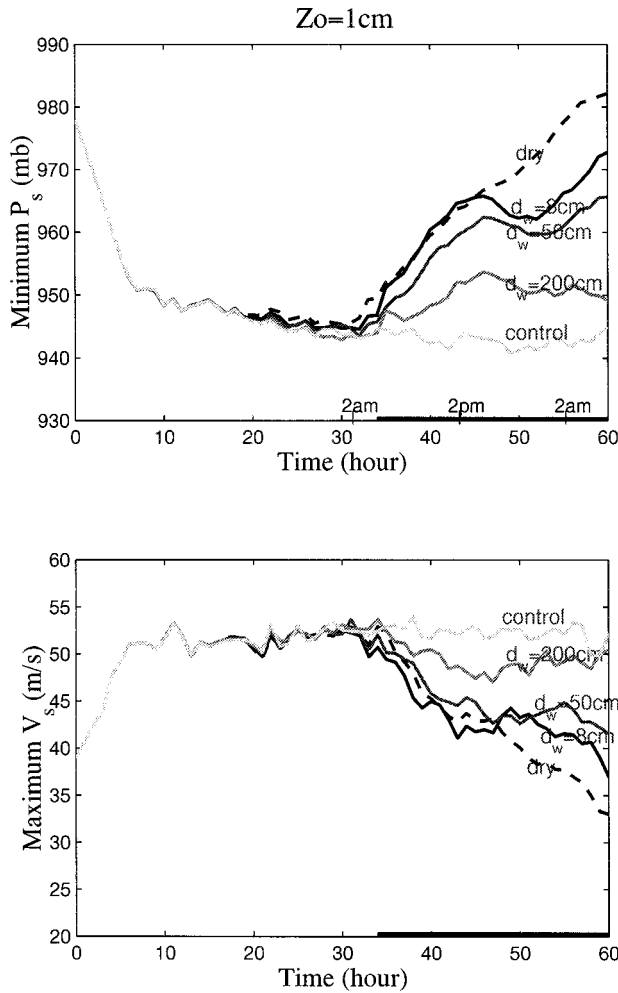
Zo=1cm

FIG. 4. Results of hurricane intensity during the 60-h integrations for different surface conditions. Surface roughness of 1 cm is used in these experiments. Here d_w is the surface water depth. The reference bars on the bottom, symbolizing the land, indicate that the hurricanes make landfall after about 34 h.

Surface temperature (°C)   35 h
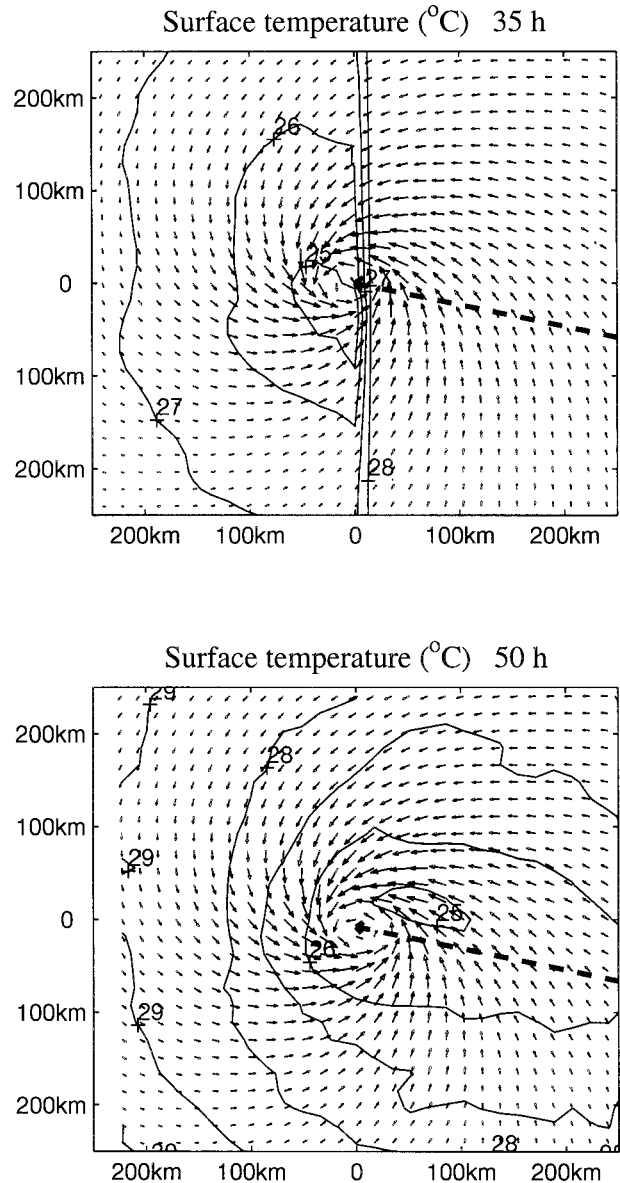

Surface temperature (°C)   50 h

FIG. 5. Land surface water temperature fields around the hurricane center (the domain of the most inner mesh is shown) in the case of $d_w = 50$ cm. The 28°C contour in the temperature field at 35 h approximately denotes the separation of land and ocean in which the surface temperature is fixed. The domain at 50 h has land surface (covered with water) everywhere. The thick dashed lines show the hurricane tracks.

the available energy considerably decreases, consistent with the intensity reduction shown in Fig. 1. Note that even the low-level increase in virtual temperature in the cutoff cases is related to the surface heat exchanges, which leads to a profile similar to that of the ascent in the storm environment (Fig. 3, circle line).

The circularly averaged vertical profiles of the θ_e and convective heating (not shown) indicate that with the underlying surface evaporation cutoffs, the convective heating is much reduced but the size of the hurricane eye remains essentially the same, implying the intense eyewall convection occurs over the area with no surface evaporation. For the control case, there is an overall θ_e increase from the ambient to the eyewall in the surface atmospheric boundary layer (Fig. 2a) though the increase is small near the surface. This overall θ_e increase in the surface boundary (convergence) layer approximately represents the energy fluxes from the ocean sur-

face because the vertical energy exchange on the top of the atmospheric boundary layer outside of the hurricane eyewall is very small (Tuleya 1991). The increase of θ_e is important for hurricane maintenance in the control case. With the underlying evaporation cutoffs, the θ_e increase in the surface atmospheric boundary layer is significantly reduced. In the case with an evaporation cutoff within $r = 200$ km, the θ_e increase nearly disappears but a storm of reduced intensity is maintained through an available energy, which is close to the en-

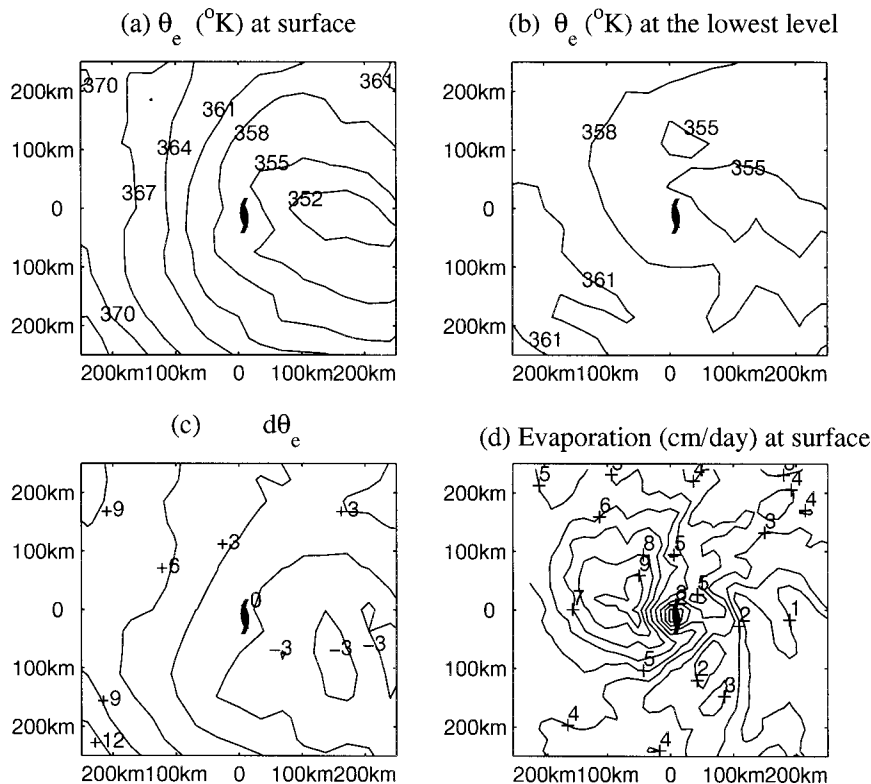FIG. 6. The θ_e distributions at (a) the surface and (b) the lowest model level, (c) their difference $d\theta_e$, and (d) the surface evaporation at 50 h for the case of $d_w = 50$ cm. The θ_e at the land water surface is computed based on the air saturated at the surface pressure and temperature.

vironmental convective available potential energy (CAPE) (see Fig. 3). Note that even in this case, the surface evaporation in the surrounding environment is important for the maintenance of both the environmental CAPE and storm circulation (see the hurricane intensity difference between the $r = 200$ km and $r = $ infinity cases shown in Fig. 1).

It is worth pointing out that some specific features of the storms in our experiments, such as the eye size and the magnitudes of the storm maintained with the surface evaporation cutoffs, may be somewhat related to the parameterizations of some physical processes used in the current GFDL hurricane model as well as the environmental conditions used in this study. For example, the cumulus parameterization by Kurihara (1973) allows substantial values of CAPE to be maintained in the atmosphere. For the experiments performed, we used the initial vertical profiles of temperature and relative humidity from GATE III tropical conditions, which have CAPE of about 1300 J kg^{-1}. With the Kurihara cumulus parameterization, this CAPE is maintained in the hurricane environment and CAPE near 2000 J kg^{-1} is also developed in some areas after a day. Although the role of environmental CAPE in determining the intensity of actual hurricanes is still debatable, we should note here that any excessive CAPE may cause less sensitivity of hurricane intensity to a given underneath surface evap-

oration reduction that will be investigated in the following sections.

4. Effects of surface water over land on landfall decay

a. Effects of hurricane-induced local surface cooling

In this section, we investigate hurricanes starting over the ocean with surface albedo of 0.06 and fixed SST of 28.5°C and making landfall (when the hurricane center encounters the shore) after about 34 h. The land surface conditions are summarized in the upper part of Table 2. Figure 4 presents the results of model-attained surface central pressures and maximum surface winds (hereafter, the wind at the lowest model level, about 40 m above ground, is referred to as the surface wind) for 60-h integrations. In all cases, a quasi-steady-state hurricane intensity related to the ocean condition is reached before hurricane landfall. Over dry land the hurricane decays very rapidly. However, the hurricane decay rate is reduced due to the presence of surface water. The decay rate is clearly dependent on the depth of the surface water. The 200-cm water layer retains a hurricane of intensity close to that in the control case as the impact of the surface flux reduction is small in this case. There are noticeable diurnal variations in the 8- and 50-cm
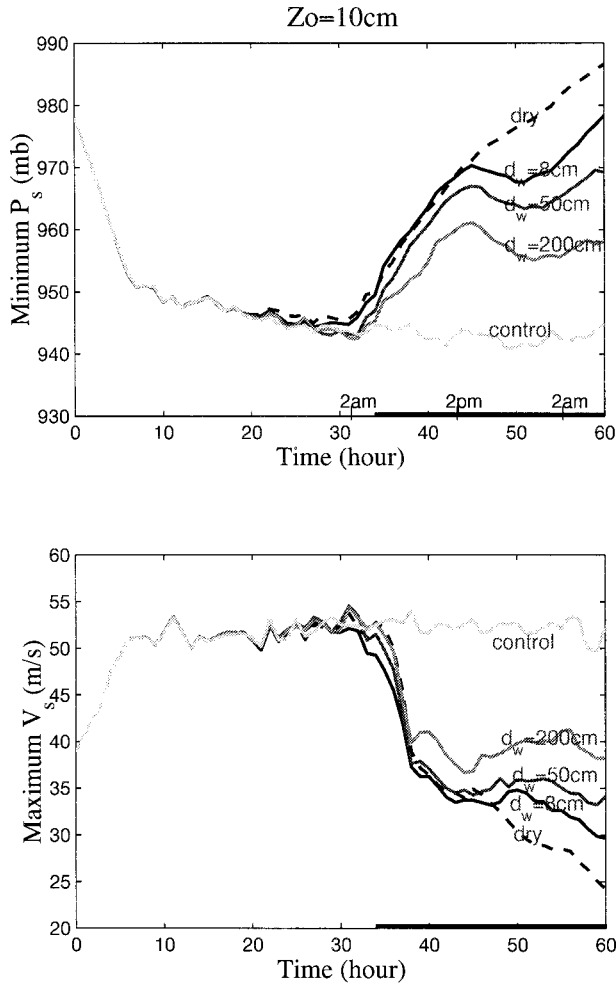
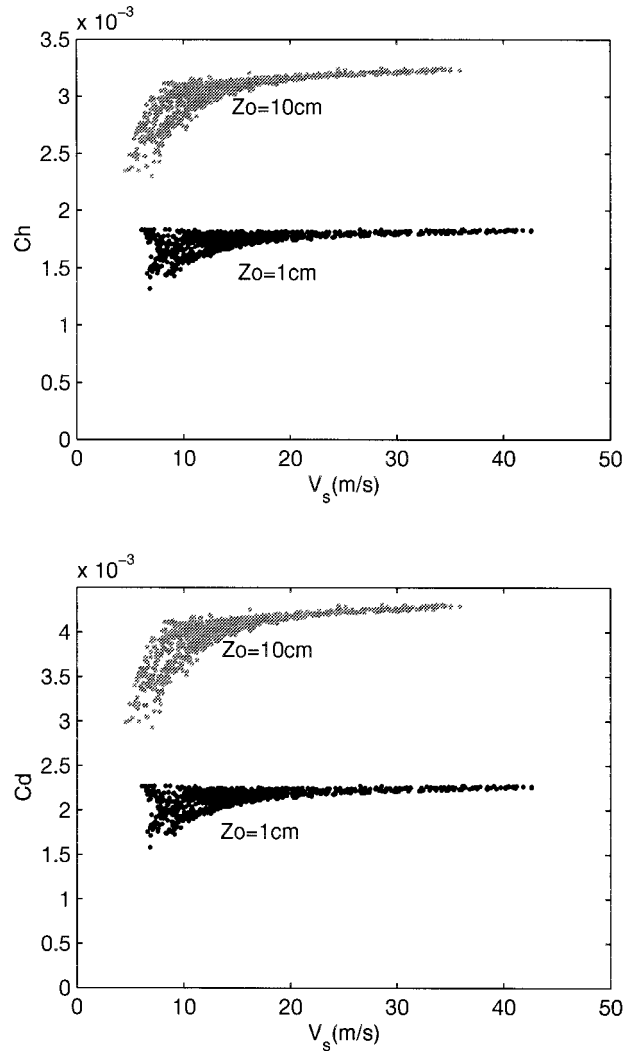FIG. 7. Same as Fig. 4 but with surface roughness of 10 cm.

FIG. 8. Momentum (Cd) and moisture (Ch) coefficient distributions with surface wind. These are the equivalent coefficients with the conventional (bulk aerodynamic) formulation used to calculate the fluxes obtained with the Monin–Obukhov scheme used in the model. Each dot denotes a grid point in the most inner mesh.

cases. The diurnal variations are large because the temperature of the subsurface layer of small heat capacity is very sensitive to the diurnal cycle of solar radiation. The diurnal variations will be further discussed in section 5.

Figure 5 shows the horizontal distributions of surface temperature at 35 h (just after landfall) and 50 h (deep inland), respectively, for the $d_w = 50$ cm case. The largest surface cooling is seen on the left side of the hurricane at 35 h while it is behind and on the right side at 50 h. The asymmetry (about the hurricane track) in the surface temperature fields at 35 h can be explained with the generally axisymmetric surface wind and pressure fields as well as the asymmetric surface conditions. The surface condition asymmetry leads to a colder surface (over land) in front of the hurricane center and a warmer surface (over ocean) behind. This surface temperature asymmetry leads to similar temperature and moisture (mixing ratio) asymmetries in the near-surface air through surface heat exchanges. Due to the near-surface hurricane circulation, the colder/drier and warmer/moister centers are shifted cyclonically. This cyclonic

shift in the near-surface air would lead to larger surface heat fluxes on the left side than on the right side of the track provided a surface temperature symmetric about the storm track. Thus, this surface temperature symmetry would be altered due to the asymmetric surface heat fluxes. Even with the cross-track surface temperature asymmetry at 35 h, less (more) temperature and moisture advections into the left (right) side and more (less) surface heat fluxes on the left (right) side are evident (not shown). In the lower panel (at 50 h), the cross-track asymmetric surface temperature may be explained with the near-surface cyclonic circulation and the phase/time-lagged local surface cooling due to hurricane movement. Note that the phase/time-lagged local surface cooling leads to a surface temperature asymmetry opposite to that at 35 h. Therefore, the cross-track
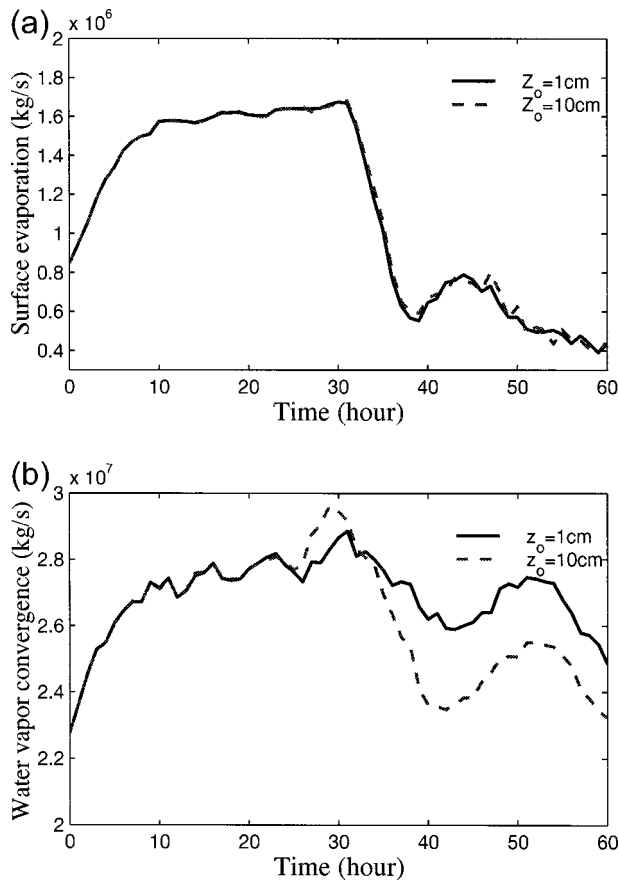
FIG. 9. (a) Surface evaporation over the area within $r = 100$ km. (b) Surface water vapor convergence into the area within $r = 100$ km for the lowest model layer (with height of 100 m).

asymmetry in the surface temperature cooling behind the hurricane center is a result of a phase-lagged surface cooling. In this case, the surface temperature around the hurricane center and eyewall is more than 4°C lower than in the environment.

Surface temperature fields at different times after landfall were examined but the patterns were found very similar to that in the 50 h case in Fig. 5 except for the diurnal variations. The cross-track asymmetric surface cooling after landfall revealed here is similar to that in the hurricane–ocean interaction case in which the surface cooling is phase-lagged with its maximum on the right side of the hurricane path (e.g., Ginis 1995). However, the mechanisms for the rightward bias of the maximum surface cooling are different, although both of them are related to hurricane movement. One important difference is that the largest cooling in the land surface water case is much closer to the hurricane center. The causes of the local surface cooling and its diurnal variation in the land surface water case will be discussed in section 5.

The 8-cm water depth case is equivalent, in terms of land thermal property, to the case investigated by Tuleya (1994) in which full surface water availability ($W = 1$)

was used for an underlying surface layer of soil. As was shown in Tuleya (1994), the largest surface cooling occured near the hurricane center. This was also confirmed in this study (not shown). In the 8-cm water depth case, the local surface temperature anomalies also indicate relatively large diurnal variations with large values during the day and small values during night.

In general, the surface temperature at a given location along the hurricane path decreases when the hurricane approaches and increases (restores to the environmental value) after the hurricane moves out. Thus, the major decrease of surface temperature at a particular location occurs during the passage of the hurricane core system (with surface wind significantly larger than in the surrounding environment). Because of the dominating role of the surface evaporation in temperature change (this will be discussed in section 5), the temperature change at a particular location mainly depends on the surface moisture disequilibrium[1] and the surface wind.

The largest cooling in the $d_w = 8$ cm case is very close to the hurricane core while the largest cooling in the $d_w = 200$ cm water case is far behind (not shown). This is consistent with the considerably smaller timescale of the temperature evolution in the shallow water case according to (1). Also related to this is the smaller horizontal scale of the major local surface cooling along the hurricane path in the shallower water case. In particular, the major local surface cooling is very much confined to the hurricane core in the 8-cm water depth case. Furthermore, the cross-track asymmetry of the surface cooling is smaller in this case. Thus, it is not only the less surface cooling but also the further-behind major surface cooling that lead to reduced effect of surface cooling on hurricane intensity in the deeper water cases.

Figures 6a and 6b show the θ_e distributions at the surface and the lowest model level, respectively, corresponding to the surface temperature field shown at 50 h in Fig. 5. The lowest surface θ_e is even further behind the hurricane center than the lowest surface temperature (Fig. 5b). This is because the surface θ_e is largely dependent on the surface saturated mixing ratio uniquely determined by the surface water temperature and pressure. Related to this surface θ_e distribution is the similar asymmetric pattern above (Fig. 6b). Figure 6c shows the θ_e difference of (a) and (b). Behind the hurricane center, there is a large region of negative values where the surface evaporation is significantly reduced (Fig. 6d). In section 5, the surface sensible heat flux will be shown to be downward and its magnitude is larger than that of the latent heat flux over this region. Figure 6d shows that the largest surface evaporation occurs around the eyewall and ahead of the hurricane center while the evaporation behind the hurricane center is negligibly small.

We examined the vertical cross section of θ_e in this

---

[1] It is defined by $r_s - r_a$ where r_s is the saturated moisture mixing ratio on surface and r_a the near-surface (the lowest model level) mixing ratio.
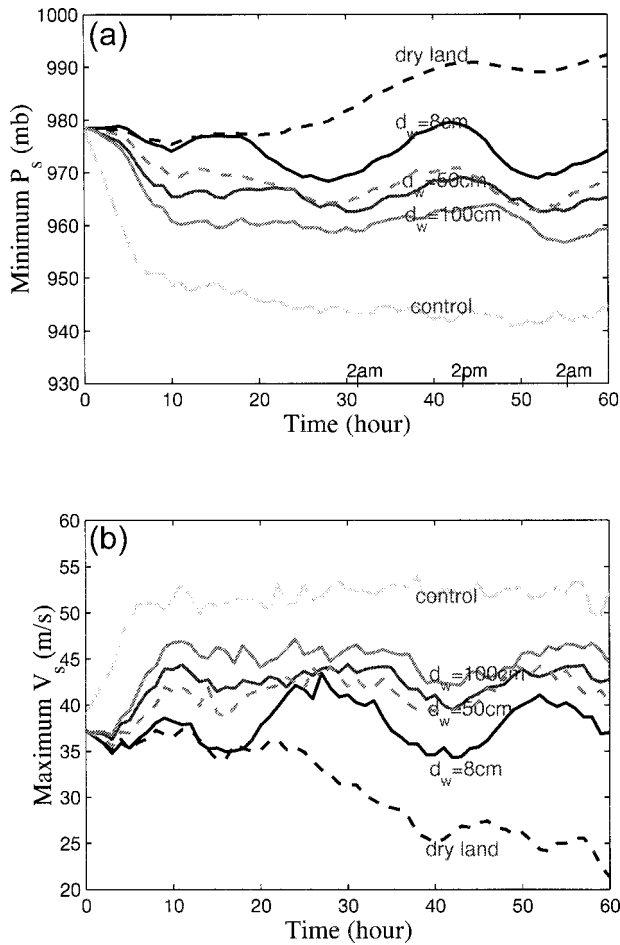
FIG. 10. Similar to Fig. 4 but for the experiments starting with land surface water conditions everywhere. The light-dashed line results from a case of an inhomogeneous surface of alternating 8- and 100-cm-deep water squares on a resolution of 1/6°.

case (not shown). In general, the θ_e near the surface is reduced due to the local surface cooling near the core region. A difference from that with the axisymmetric surface flux cutoffs discussed in the previous section is the nonaxisymmetric θ_e reduction. The largest θ_e reduction occurs behind the hurricane center due to the largest surface cooling underneath. To better understand the effects of land surface water on landfalling hurricanes, we also examined the vertical thermodynamic structures in the dry land (not shown). In the dry land case, the air in the surface boundary layer over land becomes very dry and the hurricane structure breakdown begins after landfall. The hurricane structure breakdown occurs from the lower layers to the upper layers with time.

b. Effects of surface roughness

In the experiments discussed above, a surface roughness of 1 cm (flat surface with no plants) was used with the surface fluxes calculated by the Monin–Obukhov
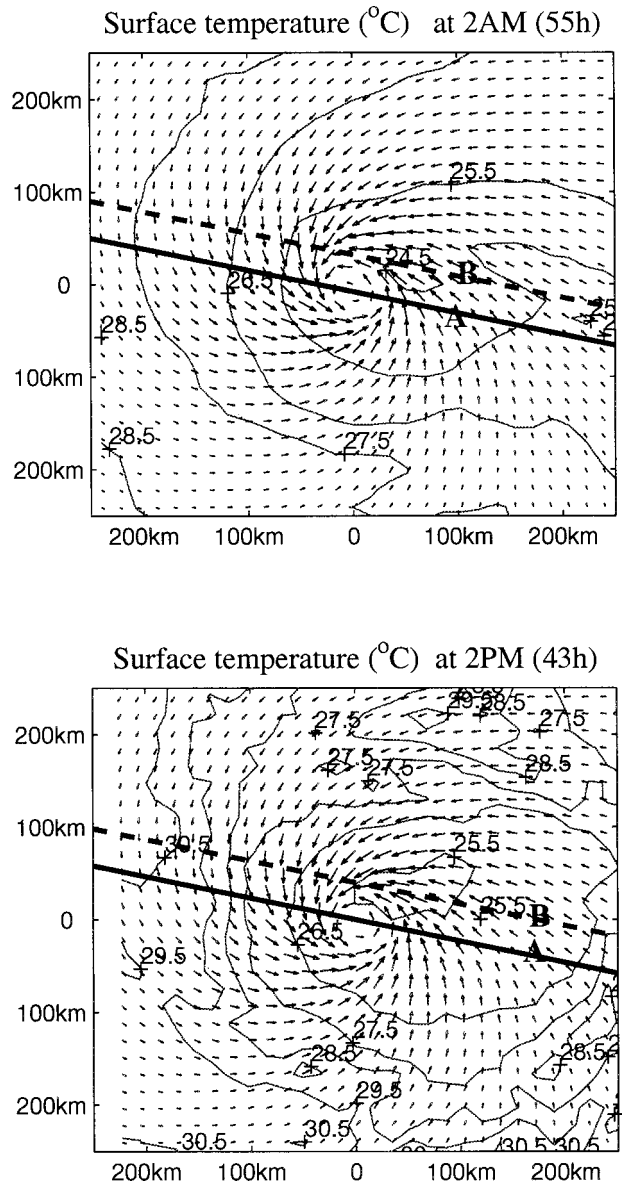
FIG. 11. Land surface water temperature fields around the hurricane core region corresponding to the case with $d_w = 50$ and $Z_o = 1$ cm shown in Fig. 10. Various surface energy fluxes are calculated along the lines A and B and are shown in Fig. 12.

scheme. In reality, however, the surface roughness may vary from region to region depending on the surface properties other than the surface water content. For simplicity, we investigate the possible effects of surface roughness on hurricane intensity change by increasing the surface roughness to 10 cm (i.e., tall grass). It is worth noting that the increase of surface roughness causes increases of both the surface heat/moisture and momentum flux exchanges. In reality, the surface moisture and momentum flux exchanges may vary from place to place. This is beyond the scope of the present study.

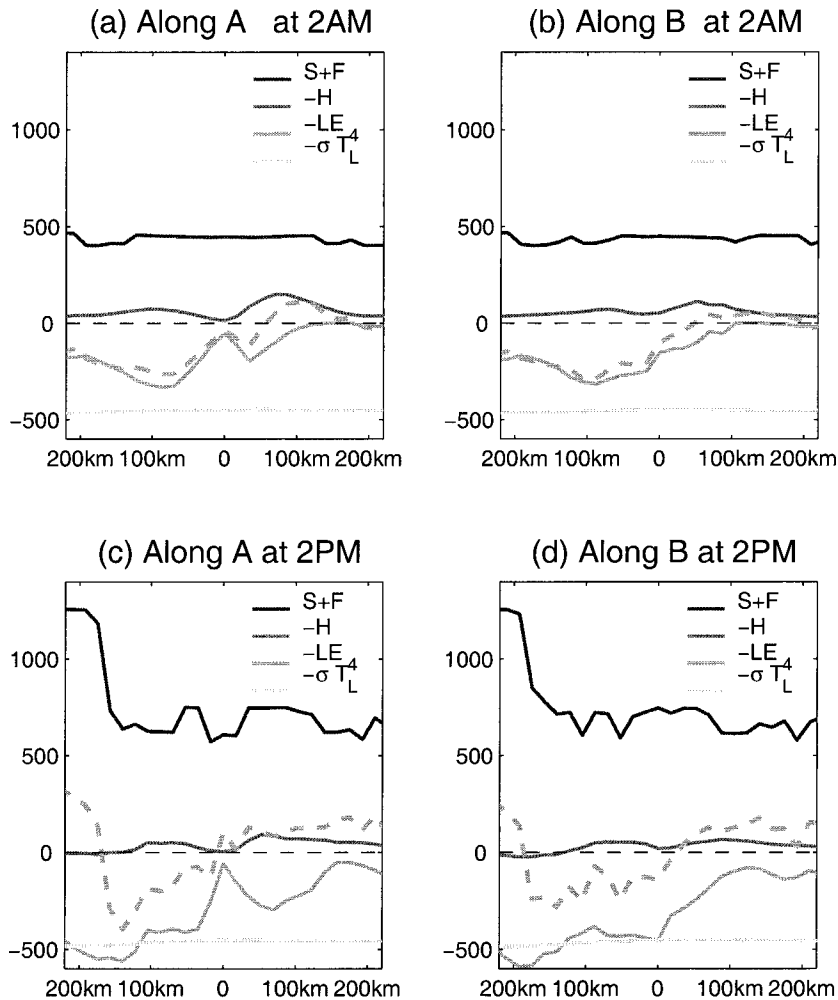Figure 7 shows the intensity changes during the 60-

FIG. 12. Surface energy fluxes (W m^{-2}) along the lines A and B in Fig. 11 from west to east. The thin dashed lines are the zero value reference lines. The thick dashed lines give the summation of all the components shown. Values less (larger) than zero denote upward (downward) energy fluxes.

h integrations for different surface water depth conditions with the surface roughness of 10 cm. According to the central pressures (Fig. 7a), the effect of the surface water on the reduction of hurricane decay rate is somewhat (but not much) reduced with the roughness increase compared to Fig. 4, while the surface winds are substantially reduced after landfall. The surface cooling and evaporation during landfall were also examined (not shown) and found to be very similar to those in the Z_o = 1 cm case shown in Figs. 5 and 6. This is probably because the increase of surface roughness leads to increase of both the momentum and moisture exchange coefficients. Figure 8 shows the equivalent momentum and moisture coefficients (see their definitions in the figure caption) as a function of surface wind in both cases of different roughness conditions at 50 h. Both the momentum and moisture coefficients are seen to be almost doubled with surface roughness increase from 1 to 10 cm.

The surface evaporation around the core region within radius of 100 km and the surface moisture convergence into this region for the lowest model layer were also calculated for both the Z_o = 1 and Z_o = 10 cm cases. Figure 9 shows their values during the entire 60-h integrations for the cases with d_w = 50 cm. Both hurricanes experience a very rapid reduction of surface evaporation starting from about 3 h before the hurricane center encounters the shore. Both evaporation and vapor convergence then exhibit some perturbations with the influence of diurnal variations. The major reduction of the surface evaporation near the hurricane core during landfall is barely affected by the surface roughness increase. This is due to the offsetting effects of the surface wind decrease and moisture exchange efficiency increase with the roughness increase. Figure 9b shows the similar tendency features for the surface moisture convergence into the eyewall region as the hurricanes make landfall but the reduction of the moisture convergence

surface temperature (^{o}C)   2AM

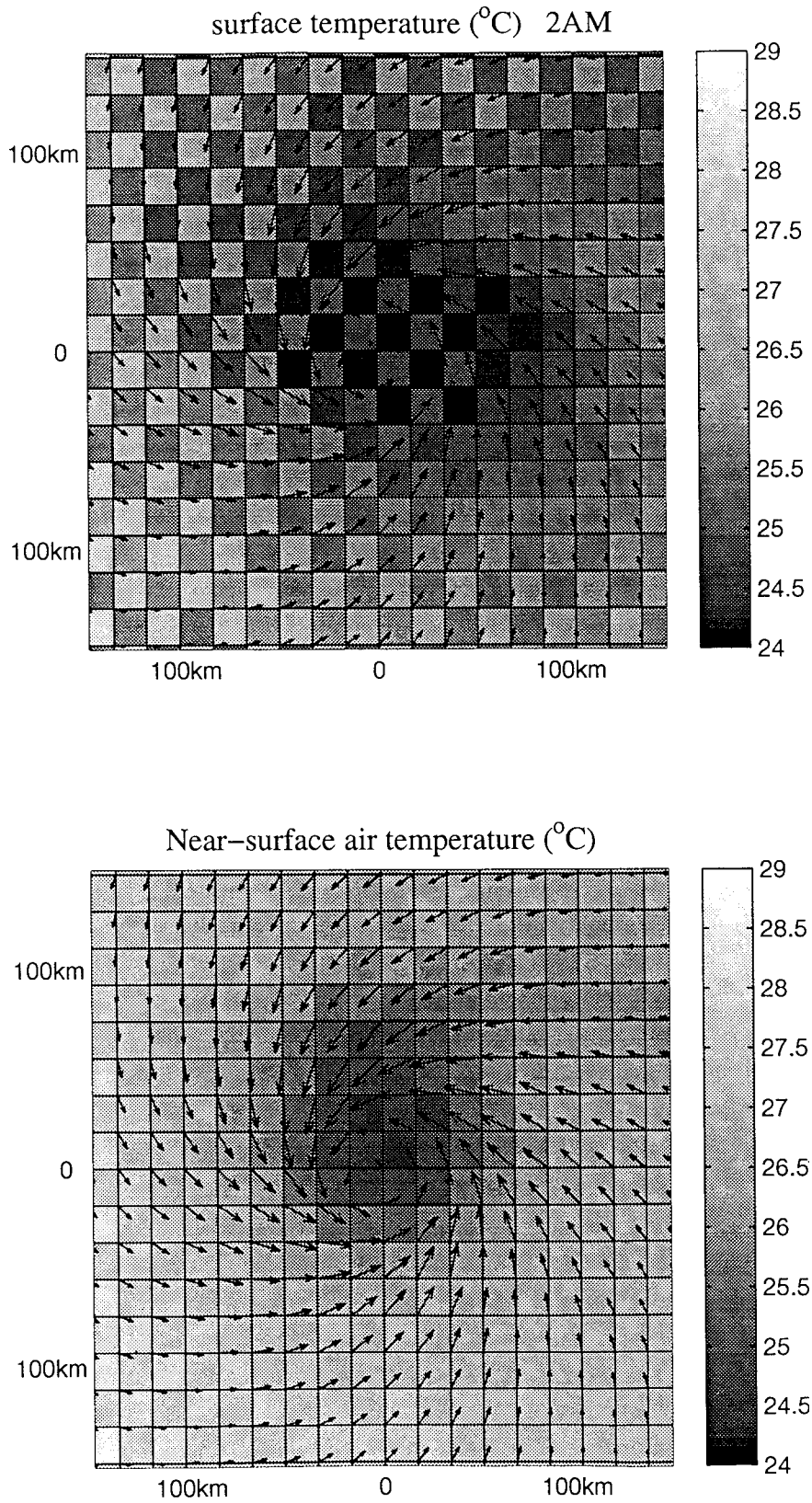Near−surface air temperature (^{o}C)

FIG. 13. Land surface water temperature and air temperature above (at the lowest model level) at 55 h for the case with the inhomogeneous surface condition corresponding to the light-dashed curve in Fig. 10.

in the $Z_o = 1$ cm case is somewhat smaller than in the $Z_o = 10$ cm case. Similar features were also found with the surface entropy convergence and eyewall convective heating (not shown). Thus, the small central surface pressure increase and convective heating reduction in the higher roughness case may be related to the smaller surface moisture and entropy convergences given the existence of CAPE and its release near the eyewall. Although only the $d_w = 50$ cm case is discussed here, similar features were also observed in the cases with $d_w = 8$ and $d_w = 200$ cm.

One can compare these idealized landfall decay rates with the empirical values of Kaplan and DeMaria (1995). In general, the decay features, such as the exponential decay during the first 10 h after landfall followed by a slower decay are in agreement. These idealized simulations of landfall may, however, underestimate observed landfall decay rates. This is because some factors, such as mountains and dry air intrusions that would augment decay rate in real cases, are not included in this study.

5. On diurnal variations of landfalling hurricanes

A set of experiments starting with land surface water conditions everywhere were also performed to study the "steady"-state hurricanes related to these conditions. Note that although these tropical systems may differ from reality due to the very idealized conditions, our goal here is to better understand the diurnal variations. In these experiments, a fixed surface roughness ($Z_o = 1$ cm) is used and the land surface water conditions used in these experiments are summarized in Table 2 (the lower part). The results of the model-attained intensity are given in Fig. 10. The slight initial maximum wind difference from the ocean control case (Fig. 10b) is because $Z_o = 1$ cm is used during the bogusing for the rest of the cases. It is apparent that considerable storm magnitudes are maintained depending on the land surface water depth, while the hurricane collapses over dry land. The intensity change in the inhomogeneous surface case with alternating 8- and 100-cm-deep waters (see the caption of Fig. 10 for more details) turns out to be quite similar to that in the 50-cm case. This case will be more discussed later in this section.

Diurnal variations of hurricane intensity are apparent in Fig. 10 with the high intensity during night and the low during the day. The diurnal variation is more significant in the shallower water case than in the deeper water case as both the environmental temperature variation and the hurricane-induced local surface cooling are larger in the shallower water case due to the smaller subsurface-layer heat capacity. One of the reasons for the diurnal intensity variation may be the cloud effects on the radiation fluxes as the clouds act to prevent the longwave radiation out and solar radiation in. But the cloud effects on solar radiation have the most significant diurnal cycle that may be mostly responsible for the diurnal intensity variation. First, the cloud effect leads

to less warming in the hurricane core than in its environment due to reduced atmospheric absorption of solar radiation in the core. This acts to reduce the warm core magnitude. Also, the cloud effect on solar radiation has its largest influence on the surface and near-surface air temperatures. It thus leads to a larger surface temperature contrast between the hurricane core region and its environment during the day (Fig. 11). This temperature contrast may lead to a similar hurricane core-environment temperature contrast aloft given the strong vertical convection and small surface thermal disequilibrium in the eyewall and the atmospheric tendency to conserve CAPE in the environment. Further examination indicates that the maximum convective heating and overall latent heat release in the eyewall are smaller during the day than during night, consistent with the intensity differences shown in Fig. 10.

To understand the causes of the local surface temperature change, we calculated all the components in (1) along line A (the hurricane path) and line B (where the lowest temperature occurs) for both the day and night situations (see Fig. 11). From a steady-state point of view, the surface energy budgets along the lines A and B from west to east represent what the surface locations on the lines experience during the hurricane passage. Due to the diurnal variations, however, these surface energy budgets may not exactly represent what the surface locations on the lines experience with time. But for the timescale of the hurricane core passage (i.e., shorter than a half-day), they approximately represent the time series pictures of the energy budget for these locations. The results of the calculations are given in Fig. 12. During night (Figs. 12a and 12b), the downward and upward longwave radiation fluxes are almost balanced. The net energy flux is primarily determined by the surface evaporation with a minor effect from the sensible heat flux, which is generally downward. Because of the small wind near the hurricane center, the evaporation there is smaller than in the surrounding areas (Fig. 12a). The energy budgets along the lines A and B show large net energy loses in front of the storm, implying large surface temperature negative tendencies. The net loses extend to the area behind the hurricane center, consistent with the largest land temperature anomaly behind the hurricane center in Fig. 11. It is also seen that the temperature is restored (on the eastern side of the cross point of the thin and thick dashed lines near the hurricane center) primarily through the sensible heat flux from the atmosphere above.

During the day, the net surface energy flux has the tendency similar to that of the surface evaporation around the core region. However, the value of net surface energy flux is generally greater than the surface evaporation due to a systematical difference between the downward and upward radiation fluxes. The evaporation is larger in this case than in the night case mainly due to the warmer surface during the day. In front of the core region, very large downward radiation fluxes are seen due to there being much less cloud there. Fur-

ther examination indicates that the largest value of the downward radiation flux seen during the day is near the clear-sky value in the surrounding environment. It is the cloud effect on the solar radiation under the hurricane core that makes the surface core–environment temperature contrast larger than in the night case. In this case, the primary restoring force is the increased daytime downward radiation fluxes (mainly the solar radiation). It should be pointed out that some small-scale features, such as the rotation of the major convective cells around the hurricane, might have affected the details in the surface energy flux distribution but were found to have little impact on the major findings outlined above.

Figure 13 shows the surface temperature and near-surface air temperature fields around the core region during night for the case with inhomogeneous water depths, an environment typical of swamps. The surface temperature primarily reflects the alternating land surface heat capacities uniquely determined by the water depths in this case. However, the near-surface air temperature does not show such a feature particularly over the regions of strong surface winds. The relatively uniform near-surface air termperature and θ_e (also examined) generally act to reduce (increase) the surface thermodynamic disequilibrium over the shallower (deeper) water. The reduced (increased) thermodynamic disequilibrium over the shallower (deeper) water leads to less (more) evaporation than would have been with a uniform water depth, and thus less (more) surface cooling. This in turn results in a reduction of surface water temperature variability in the horizontal. As a result, the hurricane intensity change in this case turned out to be near that in the $d_w = 50$ cm case. Since this study is not intended to simulate realistic cases, no more experiments with inhomogeneous surface conditions are performed. However, the case conducted here seems to suggest a nearly averaged effect of the specified inhomogeneities on hurricane intensity.

6. Summary

The role of a water-covered land in effecting landfall decay has not been investigated much. This study, using the GFDL hurricane model, investigates the effects of land surface water on landfalling hurricanes including the surface temperature changes and their influences on surface heat fluxes, hurricane structure, and intensity. A bulk subsurface-layer scheme for surface temperature prediction was used. The water depth ranging from 8 to 200 cm and different surface roughness conditions were used corresponding to a possible range of surface conditions. The results are summarized as follows:

1) During hurricane landfall over a water-covered land large local surface cooling occurs near the hurricane core region. The surface cooling pattern is similar to that in hurricane–ocean interaction as the largest surface cooling lies behind and on the right side of the hurricane. But, different from the hurricane–

ocean interaction case, the major local surface cooling can be much closer to the hurricane center and its magnitude can be larger, depending on the surface water content/depth. The larger the water depth, the further behind the largest surface cooling. The rightward bias of the largest cooling in the land surface water case is related to the hurricane movement as in the case of hurricane–ocean interaction. However, unlike over the ocean, this rightward bias is related to the asymmetry of surface evaporation about the hurricane track as a result of a phase-lagged surface cooling.

2) The local surface cooling over a water-covered land causes a reduction in potential evaporation, thereby considerably reducing hurricane intensity during landfall. The reduction depends on the depth of surface water. On the other hand, the presence of surface water makes landfall decay significantly slower than that with either dry or wet land. With a half-meter surface water layer, the temperature near the hurricane core is more than 4°C lower than in its environment. In this case, the hurricane maintains its central pressure of about 965 mb with surface roughness of 1 cm, while it would deepen to about 943 mb over an ocean and collapse over dry land.

3) An increase of surface roughness (Z_o) from 1 to 10 cm significantly reduces the surface winds but only yields a little increase in the central pressure. The major local surface cooling with the $Z_o = 1$ and 10 cm conditions is quite similar in both pattern and magnitude. This is because an increase of surface roughness enhances both the surface evaporation and the surface drag. Calculations of the surface evaporation under the hurricane core show that the values of total surface evaporation within the area of radius $= 100$ km with these different surface roughness conditions are almost the same. However, the surface moisture and entropy convergences into this area in the $Z_o = 10$ cm case are a little smaller than those in the $Z_o = 1$ cm case. This may be responsible for the small central pressure increase in the $Z_o = 10$ cm case given the existence of CAPE and its release near the eyewall.

4) Due to the small surface-layer heat capacity, the hurricane intensities exhibit noticeable diurnal variations after landfall. The amplitudes of the diurnal variations are larger for shallower waters. Hurricane intensities are relatively high during night and low during the day. With a half-meter surface water layer, the amplitude of the diurnal variation of the central pressure is about 7 mb, and about 5 m s^{-1} for the maximum surface wind. Without solar radiation during night, the surface evaporation during the passage of the hurricane core system dominates the local surface cooling. This causes a surface temperature contrast between the hurricane core region and its environment. The surface temperature contrast is enhanced during the day because of the reduction of solar radiation under the storm cloud canopy. The

cloud effect on solar radiation also leads to less warming in the hurricane core than in its environment. Both the cloud-induced temperature differences can act to reduce the hurricane warm core magnitude and circulation. This may have contributed to the diurnal variations in the hurricane intensity in this study.

5) The surface evaporation reductions under the hurricane core do not yield any large changes of the eye size although hurricane intensity is significantly reduced. Without surface evaporation reduction (fixed surface temperature), the energy input from the underlying sea surface near the core region is very important for the maintenance of hurricane of relatively high intensity. On the other hand, the considerable CAPE in the model hurricane environment may be at least partially responsible for the maintained storm magnitudes in the local surface evaporation cutoff cases. Although it is still debatable to what extent environmental CAPE controls the intensity in actual hurricanes, any excessive CAPE may cause less sensitivity of hurricane intensity to a given underneath surface evaporation reduction.

Finally, we should point out here that the equivalent water depth denoted by d_w and surface thermal properties such as the surface wetness or water availability and albedo used in this study were fixed during the model integrations. The equivalent water depth for the subsurface-layer heat capacity actually reflects both the surface water and the soil underneath in reality. Thus, the fixed equivalent water depth and surface thermal properties are poor approximations when the surface water is very shallow. This may have seriously affected the results in the cases with an 8-cm depth of surface water. For this case, the surface evaporation in reality may significantly change the heat capacity, surface water availability, and albedo. Nevertheless, with evaporation-induced surface water availability and albedo changes, the results in the 8-cm case should come close to those obtained with dry surface conditions. Rainfall can also significantly affect the local surface water content, water availability, and albedo around the hurricane core region when the land is relatively dry or has very shallow surface water. Rainfall feedback along with utilization of more advanced cumulus convection and land surface schemes, together with high-resolution experiments will be a subject of future work.

REFERENCES

Beckerle, J. C., 1974: Air and sea temperatures during traverse of Hurricane Alma 1966. *J. Phys. Oceanogr.,* **4,** 487–492.

Bender, M. A., I. Ginis, and Y. Kurihara, 1993: Numerical simulations of tropical cyclone–ocean interaction with a high-resolution coupled model. *J. Geophys. Res.,* **98** (D12), 23 245–23 262.

Black, P. G., and G. J. Holland, 1995: The boundary layer of tropical cyclone Kerry (1979). *Mon. Wea. Rev.,* **123,** 2007–2028.

Cione, J. J., and P. G. Black, 1998: Surface thermodynamic observations within the tropical cyclone inner core. Preprints, *Symp. on Tropical Cyclone Intensity Change,* Phoenix, AZ, Amer. Meteor. Soc., 141–145.

Deardorff, J. W., 1978: Efficient prediction of ground surface temperature and moisture, with inclusion of a layer of vegetation. *J. Geophys. Res.,* **83,** 1889–1903.

Emanuel, K. A., 1988: Toward a general theory of hurricanes. *Amer. Sci.,* **76,** 371–379.

——, 1995: Sensitivity of tropical cyclones to surface exchange coefficients and a revised steady-state model incorporating eye dynamics. *J. Atmos. Sci.,* **52,** 3969–3976.

Ginis, I., 1995: Ocean response to tropical cyclones. *Global Perspectives on Tropical Cyclones,* R. Elsberry, Ed., World Meteorological Organization, 198–260.

Holland, G. J., 1997: The maximum potential intensity of tropical cyclones. *J. Atmos. Sci.,* **54,** 2519–2540.

Kaplan, J., and M. DeMaria, 1995: A simple empirical method for predicting the decay of tropical cyclone winds after landfall. *J. Appl. Meteor.,* **34,** 2499–2512.

Kurihara, Y., 1973: A scheme of moist convective adjustment. *Mon. Wea. Rev.,* **101,** 547–553.

——, and M. A. Bender, 1980: Use of a movable nested mesh model for tracking a small vortex. *Mon. Wea. Rev.,* **108,** 1792–1809.

——, ——, R. E. Tuleya, and R. J. Ross, 1990: Prediction experiments of hurricane Gloria, 1985, using a multiply-nested movable mesh model. *Mon. Wea. Rev.,* **118,** 2185–2198.

——, R. E. Tuleya, and M. A. Bender, 1998: The GFDL hurricane prediction system and its performance in the 1995 hurricane season. *Mon. Wea. Rev.,* **126,** 1306–1322.

Lacis, A. A., and J. E. Hansen, 1974: A parameterization for the absorption of solar radiation in the earth's atmosphere. *J. Atmos. Sci.,* **31,** 118–133.

Mellor, G. L., and T. Yamada, 1974: A hierarchy of turbulence closure models for planetary boundary layers. *J. Atmos. Sci.,* **31,** 1791–1806.

Miller, B., 1964: A study of the filling of hurricane Donna (1960). *Mon. Wea. Rev.,* **92,** 389–406.

Ooyama, K. V., 1969: Numerical simulation of the life cycle of tropical cyclones. *J. Atmos. Sci.,* **26,** 3–40.

Price, J. F., 1981: Upper ocean response to a hurricane. *J. Phys. Oceanogr.,* **11,** 153–175.

Riehl, H., 1954: *Tropical Meteorology.* McGraw-Hill, 392 pp.

Rosenthal, S., 1971: The response of a tropical cyclone model to variations in boundary layer parameters, initial conditions, lateral boundary conditions and domain size. *Mon. Wea. Rev.,* **99,** 767–777.

Schwarzkopf, M. D., and S. B. Fels, 1991: The simplified exchange method revised: An accurate, rapid method for computation of infrared cooling rates and fluxes. *J. Geophys. Res.,* **96,** 9075–9096.

Shen, W., R. E. Tuleya, and I. Ginis, 2000: A sensitivity study of the thermodynamic environment on GFDL hurricane intensity: Implications for global warming. *J. Climate,* **13,** 109–121.

Smagorinsky, J., 1963: General circulation experiments with the primitive equations: I. The basic experiment. *Mon. Wea. Rev.,* **91,** 99–164.

Sutyrin, G. G., 1980: Response of the upper layer of the ocean to a moving typhoon. *Meteor. Hydrol.,* **9,** 48–55.

Tuleya, R. E., 1991: Sensitivity studies of tropical storm genesis using a numerical model. *Mon. Wea. Rev.,* **119,** 721–733.

——, 1994: Tropical storm development and decay: Sensitivity to surface boundary conditions. *Mon. Wea. Rev.,* **122,** 291–304.

——, and Y. Kurihara, 1978: A numerical study of the landfall of tropical cyclones. *J. Atmos. Sci.,* **35,** 242–257.

——, M. A. Bender, and Y. Kurihara, 1984: A simulation study of the landfall of tropical cyclones using a movable nested-mesh model. *Mon. Wea. Rev.,* **112,** 124–136.